Design and Evaluation of an SOI Pixel Sensor for Trigger-Driven X-Ray Readout

Ayaki Takeda, Yasuo Arai, Syukyo Gando Ryu, Shinya Nakashima, Takeshi Go Tsuru, Toshifumi Imamura, Takafumi Ohmoto, and Atsushi Iwata

***Abstract*—We have been developing a monolithic active pixel sensor with the silicon-on-insulator (SOI) CMOS technology for use in future X-ray astronomical satellite missions. This sensor is called XRPIX. Our objective is to replace the X-ray CCD, which is currently the standard detector in the field, with the developed XRPIX, which offers high coincidence time resolution (∼50 ns), superior hit-position readout time (∼10 μs), and wide bandpass (0.5–40 keV), in addition to having comparable performance in terms of imaging spectroscopy. In our previous study, we built a prototype sensor called XRPIX1 and confirmed its basic X-ray imaging spectroscopy performance in a mode that read out the entire area (all pixels). The next step is to realize a high-speed, intelligent readout for X-ray detection. XRPIX1 comprises a trigger circuit for each pixel, so as to detect an X-ray photon injection; this system is capable of direct access to selected pixels to read out the signal amplitude. We describe the design of the trigger circuitry system and report on the first resolved X-ray spectra obtained in the trigger-driven readout mode.**

***Index Terms*—Active pixel sensor (APS), correlated double sampling (CDS), intra-pixel trigger function, silicon-on-insulator (SOI) pixel sensor, X-ray astronomy.**

I. Introduction

FUTURE X-ray astronomical satellite missions will require a new type of a detector that can distinguish X-rays and charged particle tracks, so as to reduce the background level. Unfortunately, present standard detectors, i.e., the X-ray CCD [1]–[3], can not provide this capability, because of their low readout speed. The new detector must have high coincidence time resolution ($\sim$ 50 ns), superior hit-position readout time ($\sim$ 10 μs) in order to reduce a non-X-ray background by cosmic rays. In addition, it must have wide bandpass (from soft to hard X-rays, 0.5–40 keV), and comparable performance in terms of imaging spectroscopy [4], [5]. Such a detector should offer unprecedented benefits for observational studies of astronomical objects such as black holes, supernova remnants, and clusters of galaxies at long distances.

Active pixel sensors (APSs) have attracted considerable attention recently for their improved performance, which is close to that of CCDs in terms of small pixel size and low readout noise [6]–[8]. The advantage of the APS is the ability to directly access the selected pixels, which results in a faster readout. Furthermore, the APS can generate a hit timing signal instantaneously; therefore, it can achieve much better timing resolution than CCDs. Hybrid pixel sensor like Medpix [9] is one of the candidates to realize above requirements. However, the spectroscopic performance of the sensor is limited by its counting type structure, and the yield is not so good due to the large number of bump bondings. By considering the anti-coincidence between the hit signal and the external active shield detector [10], [11], the background produced by cosmic ray tracks [12] can be reduced. This is particularly important for the observation of hard X-rays with energies above 10 keV.

In order to realize the detector described above, we have been developing a new APS, called XRPIX, with the silicon-on-insulator (SOI) CMOS technology [13]. XRPIXs are monolithic pixel detectors that include a thin CMOS circuit (readout-array) layer ($\sim$ 5 μm), a buried oxide (BOX) layer (insulator of $\sim$ 200 nm), and a thick, high-resistivity Si-sensor layer (n-type, thickness 260 μm; Czochralski type, resistivity of 0.7 k$\Omega \cdot$ cm) vertically on a single chip [14] (see Fig. 1). Fig. 2 shows the concept of the XRPIX system with an active shield. The XRPIX stack is introduced to increase the quantum efficiency (depletion depth) so as to allow photoelectric absorption of hard X-rays with energies above 10 keV [15].

In our previous study [4], we presented the first prototype of the XRPIX system. The basic X-ray performance of the imaging spectroscopy was evaluated in a mode that read out the entire area (all pixels). The basic triggering operation was confirmed using laser illumination. The next step is to demonstrate high-speed, intelligent readout using X-ray irradiation. In this work, we report on the design and testing of an X-ray trigger-driven readout system for the XRPIX.

II. Device Description

A. Chip Specifications

In this paper, the evaluation results of a prototype sensor, called XRPIX1b, are presented. The sensor was fabricated using

Manuscript received June 15, 2012; revised September 09, 2012; accepted September 23, 2012. This work is supported by the KEK Detector Technology Project (DTP) and the Japan Society for the Promotion of Science (JSPS) KAKENHI under Grants 21244040 and 23340047.

A. Takeda is with the Institute of Particle and Nuclear Studies, High Energy Accelerator Research Organization, KEK, Tsukuba, Ibaraki, 305-0801, Japan, and also with the Graduate University for Advanced Studies (SOKENDAI), School of High Energy Accelerator Science (e-mail:atakeda@post.kek.jp).

Y. Arai is with the Institute of Particle and Nuclear Studies, High Energy Accelerator Research Organization, KEK, Tsukuba, Ibaraki, 305-0801, Japan (e-mail: yasuo.arai@kek.jp).

S. G. Ryu, S. Nakashima, and T. G. Tsuru are with the Department of Physics, Graduate School of Science, Kyoto University, Sakyo-ku, Kyoto, 606-8502, Japan (e-mail: ryu@cr.scphys.kyoto-u.ac.jp; shinya@cr.scphys.kyoto-u.ac.jp; tsuru@cr.scphys.kyoto-u.ac.jp).

T. Imamura, T. Ohmoto, and A. Iwata are with the A-R-Tec Corp., 10-29-1205, Saijo Otsubo-cho, Higashi-Hiroshima, Hiroshima, 739-0005, Japan (e-mail: imamura@a-r-tec.jp; ohmoto@a-r-tec.jp; iwa@a-r-tec.jp).

Color versions of one or more of the figures in this paper are available online at http://ieeexplore.ieee.org.

Digital Object Identifier 10.1109/TNS.2012.2225072

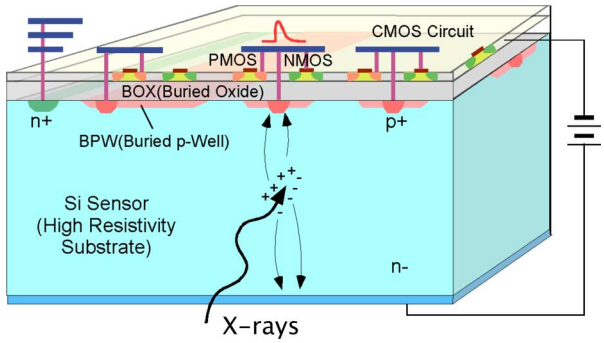

Fig. 1. Cross sectional view of the SOI pixel detector.

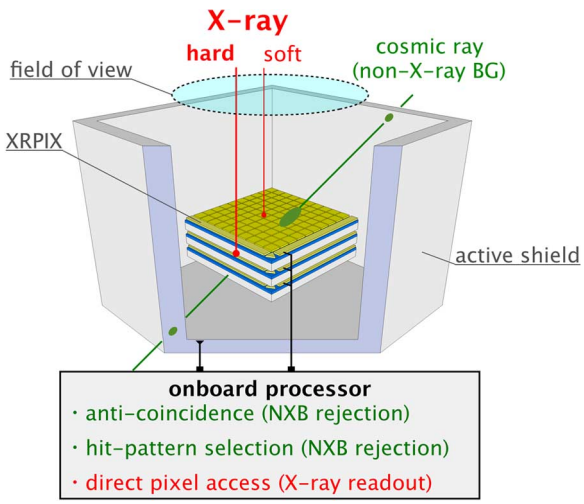

Fig. 2. Concept of an active shield system with XRPIX to reduce the non-X-ray background (NXB) by cosmic rays. The active shield can be a scintillation counter (e.g., a BGO) read out by avalanche photodiodes (APDs).

the 0.2 μm fully depleted SOI CMOS pixel process by LAPIS Semiconductor Co., Ltd. It is 2.4 mm×2.4 mm in size and consists of 32×32 pixels. The pixel size is 30.6 μm × 30.6 μm, so the effective sensing area is approximately 1.0 mm × 1.0 mm.

The sensor format and block diagram are shown in Fig. 3. For the sake of comparison and evaluation, the chip contains four different types of test element group (TEG) pixels. Each TEG have the same basic circuit, but uses different types of transistors and capacitors. The results in this paper are for the TEG constructed using body-tie transistors and metal-insulator-metal (MIM) capacitors [4], [14] which showed best performance within the 4 TEGs.

B. Pixel Circuitry and Layout

The pixel circuitry and layout of XRPIX1b are shown in Figs. 4 and 5, respectively. The pixel circuitry can be divided into two main parts: the signal processing part, containing the correlated double sampling (CDS) circuit, and the trigger part. The CDS circuit suppresses the kTC reset noise in the sense-node and subtracts the offset levels. Details of the CDS function are explained and reported in [4].

The trigger circuit generates a trigger signal when an X-ray signal crosses the threshold voltage (VTH) of the pixel. This function is realized by two inverter-chopper type comparators.

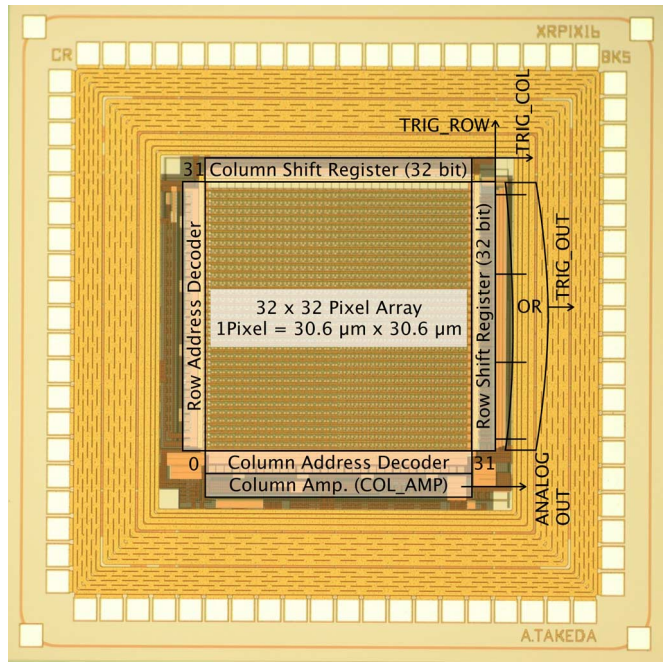

Fig. 3. XRPIX1b chip photograph and block diagram. The chip size is 2.4 mm × 2.4 mm.

The reason for using two inverter stages is for raising detection sensitivity. This comparator contains a cascade of inverter stages which is essentially a bistable multivibrator [16]. The trigger operation consists of a resetting phase and a waiting phase. The timing diagram of the trigger circuit is shown in Fig. 6. In the resetting phase, the threshold voltage is connected to the input of the trigger circuit by asserting a VTH_RST signal and stored in the capacitors (COMP Cap.1 and COMP Cap.2) by turning on and off the reset switches (RST_COMP1 and RST_COMP2) in series. Then, the VTH level is set at the input-node of the comparator. After releasing the reset signal of the sense-node (PD_RST), the input-node level of the comparator moves down to the level corresponding to the CDS_RST to allow some room for the noise not to trigger the comparator. And then, the waiting phase begins, during which the trigger output signal is asserted when the voltage at the sense-node exceeds the threshold voltage by X-ray signal.

The trigger output signal from a pixel is wired-OR'ed in the row and column directions and stored in shift registers at the edges of the sensor array. The 32 wired-OR'ed row signals are then OR'ed again, and the final trigger signal is fed to the output by the sensor. After receiving the trigger output signal with an external circuit, the store switch (STORE) is turned off. The X and Y addresses of the hit pixel are available from the row and column shift registers.

C. Hardware System for Evaluation

We have developed a compact evaluation system, as shown in Fig. 7. The system consists of the chip-loaded sub-board and the main board (SEABAS: Soi EvAluation BoArd with Sitcp, [13]). The SEABAS contains two FPGAs (Xilinx Virtex-4). One is used for chip control and data taking (called USER FPGA), and the other is used for data transmission via 100 Base-T Ethernet

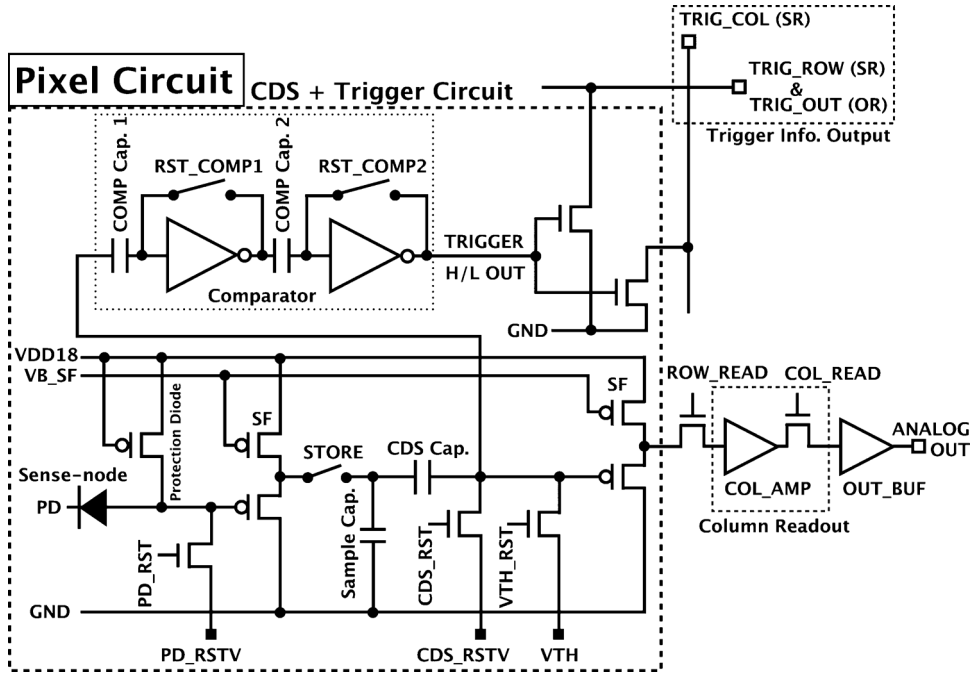

Fig. 4. Pixel circuit of the XRPIX1b. The comparator for trigger detection is an inverter-chopper type.

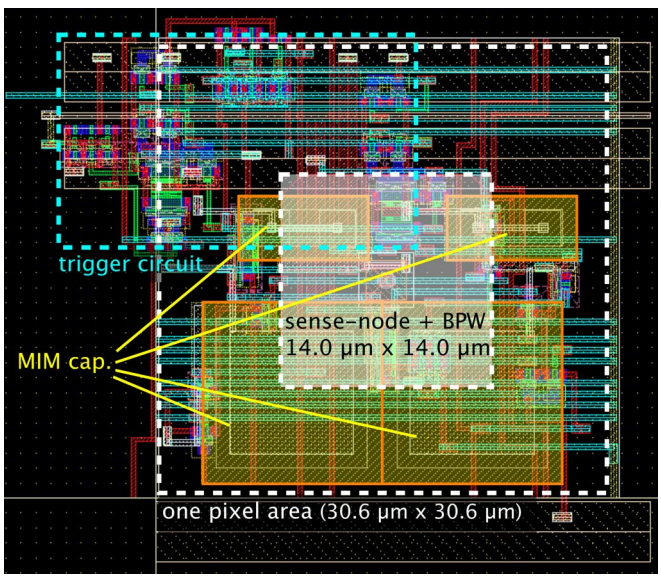

Fig. 5. Pixel layout of the XRPIX1b.

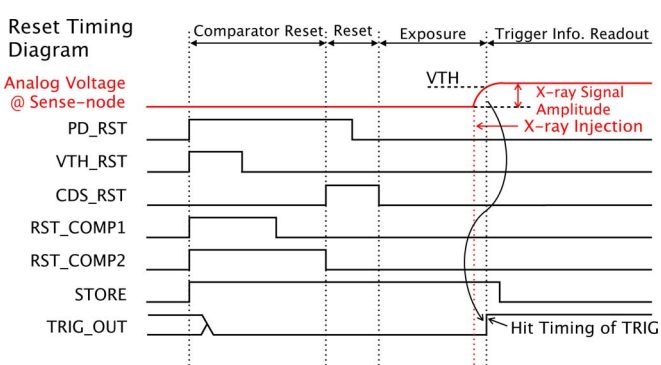

Fig. 6. Pixel operation timing diagram.

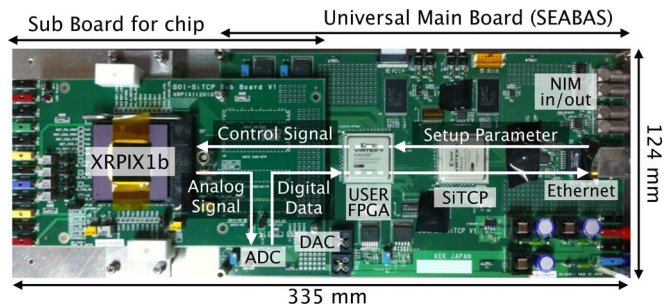

Fig. 7. General data acquisition system for SOI detectors, "SEABAS".

(called SiTCP [17] FPGA). The external clock frequency sent to the USER and the SiTCP FPGAs is 25 MHz; this frequency can be multiplied within the internal PLL circuit. The SEABAS also provides an ADC (1 V/12 bits) for pulse height digitization, a 4-channel DAC (12 bits/1.8 V) for producing reference voltages (e.g., PD_RSTV, CDS_RSTV, and VTH in Fig. 4), 2 inputs and 2 outputs of the NIM signal for communication with external modules, and a power system (±5 V inputs).

III. Readout Architecture and Data Acquisition

We have designed an intelligent readout mode driven by the pixel trigger. Figs. 8 and 9 show the flow chart and the overall timing diagram of the signals controlled by the USER FPGA, respectively.

As shown in Fig. 8, when an X-ray signal is detected by a pixel (i.e., a hit pixel, (i)), the comparator output of the hit pixel (ii) and TRIG_OUT of the 32 wired-OR'ed in row (iii) become high. Thus, USER FPGA is notified of the arrival of an X-ray and reads the hit pattern information from the row and column shift registers (iv). Thereafter, the USER FPGA accesses the hit pixel directly (v) and reads out the analog voltages (signal

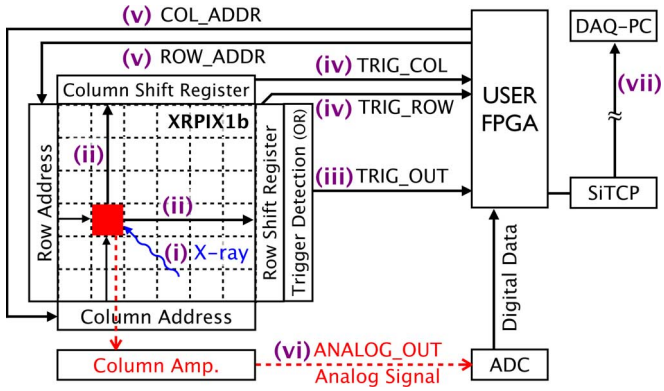

Fig. 8. Flow of the trigger-driven readout. The solid/dashed arrows show digital/analog signals, respectively.

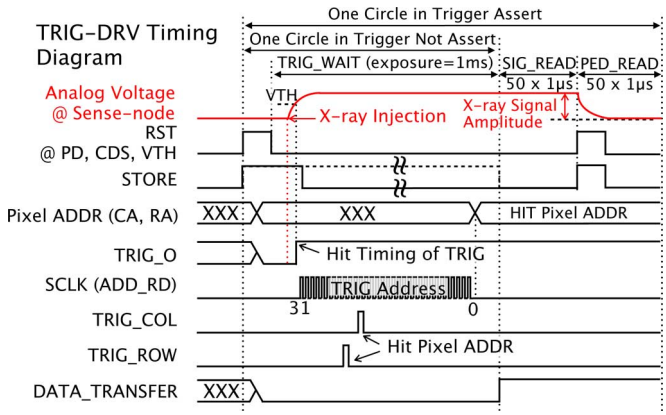

Fig. 9. Timing diagram of XRPIX1b in trigger-driven mode. The solid line shows the case of trigger assertion, and the dashed line shows the case of no trigger assertion.

and pedestal levels) using the ADC (vi). Finally, the obtained digital data is transmitted to the DAQ-PC (vii); this is called the "Trigger Assert" state. The system is reset periodically if no X-ray is detected (i.e., the "Trigger Not Assert" state).

Currently, one set of the event data contains a header (2 bytes), an event number (4 bytes), a hit timing (6 bytes), row and column addresses of the hit pixel (2 bytes), pulse height words of the signal (50 samples, 100 bytes), and pedestal levels (50 samples, 100 bytes). The total data size is 214 bytes, and the readout time is about 100 μs. The data is transferred as an 8-bit (byte) unit via 100 Base-T Ethernet.

The X-ray signal amplitude is calculated from the difference between the averages of the signal and the pedestal levels (c.f Fig. 9). This over sampling process works as a low-pass filter, reducing white noise and quantization noise.

IV. Evaluation Results

A. X-ray Responsivity Without Using Trigger-Driven Mode

Here, we describe the X-ray responsivity when reading out the entire area without using the trigger-driven mode. In this test, the sensor is biased to 100 V and is cooled to -50°C so as to suppress the dark current. Fig. 10 shows the spectrum of the X-ray emission from a ^{109}Cd radio isotope sample. The energy resolution is about 0.7 keV FWHM at 22.2 keV $(\mathrm{Ag}-\mathrm{K}_{\alpha})$. Then, the readout noise can be calculated to be about 70 electrons rms.

Fig. 11 shows the plot of X-ray energy calibration using Cu, Mo, and ^{109}Cd X-ray lines at 8 keV ($\mathrm{Cu}-\mathrm{K}_{\alpha}$ and K_{β}), 17.4 keV $(\mathrm{Mo}-\mathrm{K}_{\alpha})$, 22.2 keV, and 24.9 keV $(\mathrm{Ag}-\mathrm{K}_{\beta})$. The energy resolution is 1.0 keV FWHM at 8 keV $(\mathrm{Cu}-\mathrm{K})$. It is poor compared to the result for the ^{109}Cd because in this case $\mathrm{Cu}-\mathrm{K}_{\alpha}$ and K_{β} lines could not be separated. The energy resolution value is used for comparison with the trigger-driven mode described in Section IV-B. The ADC gain is 6.94 (ADU/keV), based on the slope of the linear fitting. In silicon, 274 electron-hole pairs are generated on the average at an X-ray energy of 1 keV. As a result, the total gain of the sensor is $6.94\ (\mathrm{ADU/keV}) \times 244(\mu\mathrm{V}/ADU)/274(\mathrm{e}-/\mathrm{keV}) = 6.18\ (\mu\mathrm{V/e}-)$.

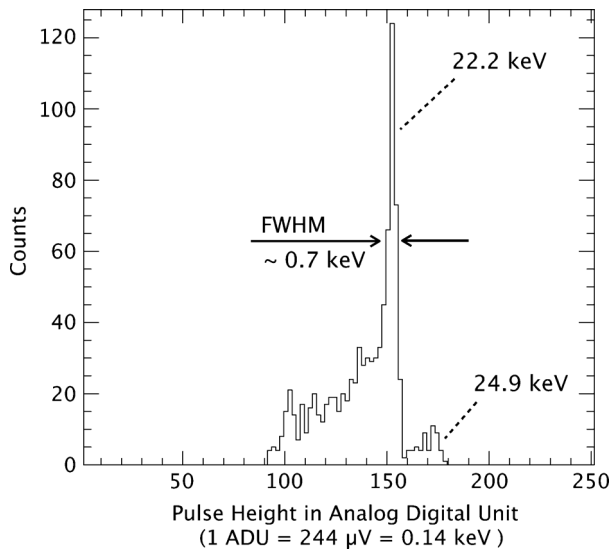

Fig. 10. X-ray pulse height in analog digital unit (ADU) of the ^{109}Cd radio isotope obtained in all pixel mode.

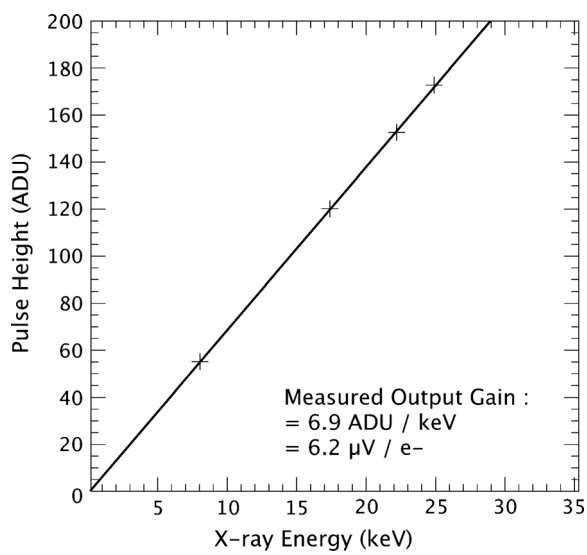

Fig. 11. Calibration between X-ray energy and signal pulse height.

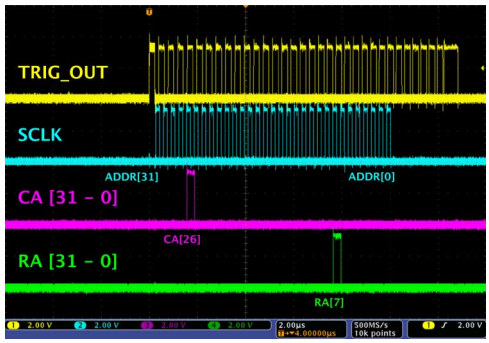

Fig. 12. Raw X-ray trigger signals recorded by the oscilloscope (c.f Fig. 9).

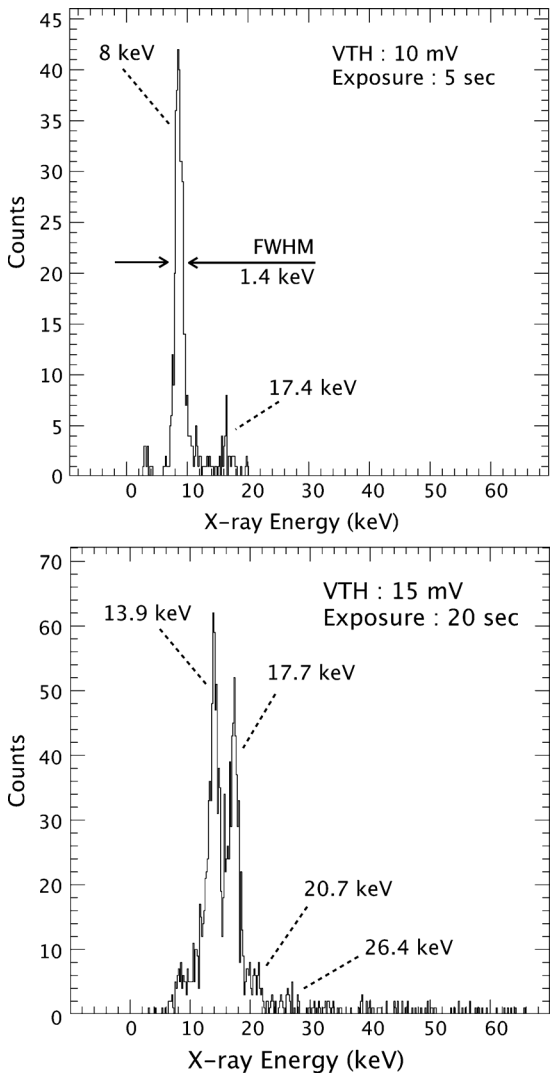

Fig. 13. X-ray spectra of the Cu+Mo target (top) and the $^{241}\mathrm{Am}$ radio isotope (bottom) obtained in the trigger-driven mode.

B. Verification in X-ray Trigger-Driven Mode

We performed X-ray irradiation tests so as to characterize the trigger-driven mode. This test was carried out under the same temperature and back bias voltage (VBack) as used in Section IV-A.

We successfully observed the X-ray trigger waveform (Fig. 12) on an oscilloscope. This figure shows the oscillation in the TRIG_OUT signal. This is probably because the TRIG_OUT signal is affected by the SCLK signal through capacitive coupling of the signals.

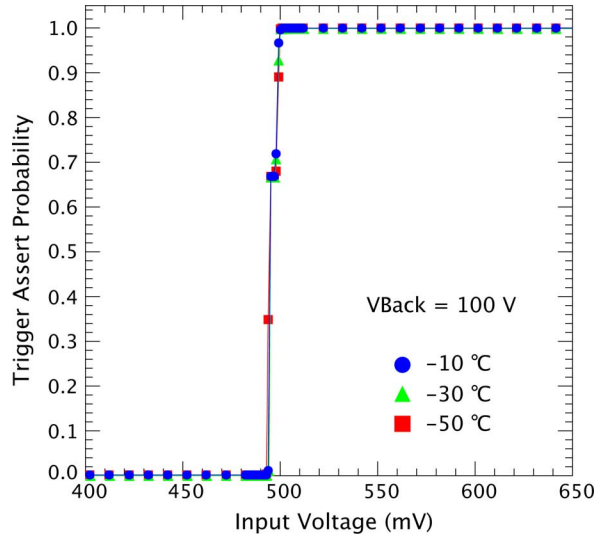

Fig. 14. Dependence of the trigger output on the input signal at a fixed threshold voltage of 500 mV. The trigger assert probability is calculated from the fraction of trigger-on events after 10000 tests at the corresponding input voltage. There was little difference when the temperature was changed from $-10^{\circ}\mathrm{C}$ to $-50^{\circ}\mathrm{C}$.

Fig. 13 shows the first resolved X-ray spectra of the Cu+Mo target and the $^{241}\mathrm{Am}$ radio isotope obtained in the trigger-driven mode. The energy resolution is 1.4 keV FWHM at 8 keV. This result indicates that the X-ray trigger-driven mode successfully resolves X-ray spectra, although the energy resolution is noticeably worse than that of the non-trigger-driven mode. This might be due to interference between the trigger circuit and the signal readout circuit.

C. Trigger Sensitivity for Low-Energy X-rays

The trigger sensitivity for the detection of low-energy X-rays is determined primarily by the circuit noise level. If the threshold level is lowered close to the noise level, the trigger output would be turned high by the noise (a false detection). To measure that limit, we supplied an input voltage from the CDS_RSTV input and observed the trigger output at a fixed threshold voltage. The STORE switch (Fig. 4) is turned off in this test to prevent the effects from the sense-node. The measurements were performed at -10, -30, and $-50^{\circ}\mathrm{C}$.

As shown in Fig. 14, there was a 1% trigger probability at a signal level of -6 mV below the threshold level at $-50^{\circ}\mathrm{C}$. This voltage corresponds to the low-energy limit of 3.5 keV, according to the calibration shown in Fig. 11.

V. Conclusions

We have developed a trigger-driven readout system in an X-ray sensor system, XRPIX1, for use in future astronomical satellite missions. We successfully demonstrated the acquisition of X-ray spectra in trigger-driven mode. To the best of our knowledge, this is the first report on the realization of an X-ray integration-type active pixel sensor that uses an intra-pixel trigger. The current low-energy limit by the trigger-driven

mode is 3.5 keV. In order to lower the threshold level and detect low-energy X-rays, we are planning to develop thin back side window process, low noise readout circuit by introducing a charge amplifier instead of the present source follower.

ACKNOWLEDGMENT

The authors acknowledge the valuable advice and great work by the personnel of LAPIS Semiconductor Co., Ltd. This work is supported by JSPS KAKENHI (21244040 and 23340047). This work is also supported by VLSI Design and Education Center (VDEC), the University of Tokyo in collaboration with Synopsys, Inc., Cadence Design Systems, Inc., and Mentor Graphics, Inc.

REFERENCES

[1] G. P. Garmire, M. W. Bautz, P. G. Ford, J. A. Nousek, and G. R. Ricker, Jr, "Advanced CCD imaging spectrometer (ACIS) instrument on the chandra X-ray observatory," *Proc. SPIE*, vol. 4851, pp. 28–44, 2003.

[2] L. Strüder *et al.*, "The european photon imaging camera on XMM-newton: The pn-CCD camera," *Astron. Astrophys.*, vol. 365, no. L18, 2001.

[3] K. Koyama *et al.*, "X-ray imaging spectrometer (XIS) on board suzaku," *Pub. Astron. Society Jpn*, vol. 59, pp. S23–33, 2007.

[4] S. G. Ryu *et al.*, "First performance evaluation of an X-ray SOI pixel sensor for imaging spectroscopy and intra-pixel trigger," *IEEE Trans. Nucl. Sci.*, vol. 58, no. 5, pp. 2528–2536, 2011.

[5] S. Nakashima *et al.*, "Progress in development of monolithic active pixel detector for X-ray astronomy with SOI CMOS technology," *Phys. Procedia DOI: 10.1016/j.phpro.2012.04.100*, vol. 37C, pp. 1392–1399.

[6] G. Prigozhin *et al.*, "Characterization of three- dimensional-integrated active pixel sensor for X-ray detection," *IEEE Trans. Nucl. Sci.*, vol. 56, no. 11, pp. 2602–2611, 2009.

[7] N. Wermes *et al.*, "New results on DEPFET pixel detectors for radiation imaging and high energy particle detection," *IEEE Trans. Nucl. Sci.*, vol. 51, no. 3, pp. 1121–1128, 2004.

[8] R. Ballabriga, M. Campbell, E. H. M. Heijne, X. Llopart, and L. Tlustos, "The Medipix3 prototype, a pixel readout chip working in single photon counting mode with improved spectrometric performance," *IEEE Trans. Nucl. Sci.*, vol. 54, no. 5, pp. 1824–1829, 2007.

[9] R. Plackett *et al.*, "Current status of the Medipix2, timepix, Medipix3 and Timepix2 pixel readout chips," *PoS, VERTEX 2010, 030*, 2010.

[10] T. Takahashi *et al.*, "Hard X-ray Detector (HXD) on Board Suzaku," *Pub. Astron. Society Jpn*, vol. 59, pp. S35–51, 2007.

[11] M. Kokubun *et al.*, "In-Orbit Performance of the Hard X-ray Detector on Board Suzaku," *Pub. Astron. Society Jpn*, vol. 59, pp. S53–71, 2007.

[12] T. Anada, T. Dotania, M. Ozaki, and H. Murakami, "Instrumental background of the X-ray CCD camera in space: Its dependence on the configuration parameters of CCD," *Proc. SPIE*, 2008, 7011, 70113X doi:10.1117/12.788138..

[13] SOIPIX Collaboration [Online]. Available: http://rd.kek.jp/project/soi/.

[14] Y. Arai *et al.*, "Development of SOI pixel process technology," *Nucl. Instrum. Meth.*, vol. 636, no. 1, Supplement 1, pp. S31–S36, 2011.

[15] M. Kokubun *et al.*, "Hard X-ray imager (HXI) for the ASTRO-H mission," *Proc. SPIE*, 2010, 7732, 773215 doi:10.1117/12.857933..

[16] R. Gregorian and G. C. Temes, *Analog MOS Integrated Circuits for Signal Processing*. Hoboken: A Wiley-Interscience Publication, 1986, pp. 425–437.

[17] T. Uchida, "Hardware-based TCP processor for gigabit Ethernet," *IEEE Trans. Nucl. Sci.*, vol. 55, no. 3, pp. 1631–1637, 2008.